

Effects of Heat Treatment on the Tribological and Corrosion Properties of Electrodeposited Ni-P Alloys.

*D. Nava, C.E. Dávalos, A. Martínez-Hernández, F. Manríquez, Y. Meas, R. Ortega-Borges, J.J. Pérez-Bueno, G. Trejo**

Laboratory of Composite Materials and Functional Coatings. Center for Research and Technological Development in Electrochemistry (CIDETEQ). Parque Tecnológico Sanfandila, Pedro Escobedo, A.P. 064, C.P. 76703, Querétaro, México.

*E-mail: gtrejo@cideteq.mx

Received: 15 October 2012 / *Accepted:* 5 November 2012 / *Published:* 1 February 2013

This paper describes the effects of heat treatment on the electrochemical behavior and tribological characteristics of Ni-P (10.65 at.% P) composite coatings. The deposits were obtained via electrodeposition onto an AISI 1018 steel electrode and then heat treated at various temperatures ranging from 200 to 600 °C for 60 min in air. The tribological characteristics studied included hardness, friction coefficient, and wear resistance. Polarization curves were used to evaluate the electrochemical behavior (corrosion resistance) of the coatings. The results indicated that the Ni-P alloy (10.6 at.% P) was originally amorphous and was transformed into a mixture of amorphous and crystalline phases when was thermally treated in the range from 400 to 500 °C. This phase transformation was associated to with the precipitation of a mixture of Ni₃P intermetallic compound and pure Ni crystals. In addition, the results showed that the wear resistance of the Ni-P coating (10.6 at.% P) increased with hardness. The maximum hardness (990 Hv) was obtained when the Ni-P coatings (10.6 at.% P) were thermally treated at 500 °C. The corrosion current density of the coatings also increased with increasing annealing temperature.

Keywords: Electrodeposition, corrosion, heat treatment, microhardness, Ni-P coatings, wear resistance

1. INTRODUCTION

Over the last two decades, a variety of surface engineering processes have been developed to enhance the wear resistance, hardness, and corrosion performance of materials. Today, Ni-P alloys are widely used in the aerospace, automotive, and electronic industries because they possess a high degree of hardness, wear resistance, and corrosion resistance, as well as a low friction coefficient [1-4]. Due to their unique properties, research on the deposition mechanism and characterization of Ni-P coatings

has increased considerably. In this regard, Malfatti et al. [5] found that the transition from crystalline to amorphous structures occurs progressively over the range of several atomic percent of phosphorous and that as deposited Ni-P coatings are amorphous when the phosphorous content exceeds 15 at.%. By contrast, the amorphous alloys can be crystallized via heat treatment followed by decomposition to Ni₃P and face-centered cubic (fcc) nickel crystals at temperatures above 350 °C [6]. The physical characteristics of the Ni-P coatings can generally be improved via an appropriate heat treatment [7-11], which can be attributed to precipitation of fine Ni crystallites and hard intermetallic Ni₃P particles during the crystallization of the amorphous phase [12]. In this respect, the wear resistance of the Ni-P alloys increases after heat treatment [8]. Moreover, it has been reported that nanocrystalline Ni-P coatings with a P content of only 2-8% exhibit a significantly higher wear resistance than coatings with a higher P content [9].

In addition, several studies have shown that Ni-P alloys are good anticorrosive coatings for several media [13-16], for these applications the phosphorus content of a Ni-P coating plays an important role in its passivity [1,17-19] and in consequence in its protection capacity. In a brine-fog study, Bai et al. [20] found that the weight loss of the Ni-P coatings decreased with increasing phosphorous content. Moreover, Wang et al. [21] recently showed that Ni-P electroless coatings heat-treated at 400 °C exhibited corrosion resistances over two orders of magnitude better than hard Cr deposits.

The aim of this work was to study the effects of heat treatment on the physical properties of electrodeposited Ni-P coatings, such as their crystalline structure, hardness, and resistance to wear and corrosion.

2. EXPERIMENTAL PART

Ni-P electrodeposits were obtained from a modified Watts nickel baths containing 0.15 M H₃BO₃, 2 M NaCl, 0.65 M NiSO₄·6H₂O, 0.75 M NiCl₂·6H₂O, and 0.10 M H₃PO₃ with a pH of 1.5 adjusted with 1 M HCl (solution S). These solutions were prepared immediately prior to each experiment using deionized water (18 MΩ cm) and analytical grade reagents of the highest purity available (Sigma-Aldrich).

To analyze the corrosion process via polarization curves and to characterize the Ni-P coatings, Ni-P coatings (10.6 at.% P) were prepared from solution S on AISI 1018 steel electrodes with a geometric area of 1 cm² enclosed in Teflon. The Ni-P (10.6 at.% P) coatings were obtained via electrodeposition of solution S under galvanostatic conditions: $i = 30$ mA and $t = 15$ min. The coating thickness was approximately 10 μm. The Ni-P coatings were then annealed in air for 60 min at one of five temperatures (i.e., 200, 300, 400, 500, or 600 °C). The electrochemical experiments were conducted with an EG&G Princeton Applied Research Potentiostat/Galvanostat (Mod. 273A) coupled to a personal computer equipped with EG&G M270 software for data acquisition.

An atomic force microscope (AFM) (Digital Instruments, Mod. Nanoscope E) was used in contact mode to image the deposited nickel on the steel substrate. These measurements were performed in air (ex-situ) using silicon nitride AFM tips (Digital Instruments). All images were

obtained at 2 Hz and are represented in the so-called height mode, in which the highest portions appear brighter. The morphology of each coating was evaluated by scanning electron microscopy (Jeol Mod. DSM-5400LV), and the topography was analyzed with a profilometer (Veeco, Mod. Dektak 6M). The deposited phases were identified via X-ray diffraction (XRD) using a Bruker diffractometer (Mod. D8 Advance) (Bragg-Brentano arrangement) with Cu $K\alpha$ -radiation ($\lambda = 1.54 \text{ \AA}$). The range of 2θ from 40° to 95° was recorded at a rate of 0.2° s^{-1} . The elemental composition of the coatings, as a function of the thickness was obtained using a glow discharge spectrometer (GDS) (Leco, Mod. 850A). The hardness was measured with a Matsuzawa MXT-ALFA Vickers microhardness tester with a 10 g load applied for 15 s. The final value quoted for the coating hardness was the average of ten measurements.

Wear tests were performed on a reciprocating ball-on-disk tribometer (CSM tribometer) in air at a temperature of approximately 25°C and relative humidity of approximately 39% under dry, non-lubricated conditions. Balls (3 mm diameter) made of AISI 8620 with a hardness of 25 HRC were used as the counter body in the wear tests. All wear tests were performed under a 1 N load at a sliding speed of 1 cm s^{-1} . The friction coefficient and sliding time were automatically recorded during the test. The wear volume was measured according to the ASTM G99 standard method. Three wear tests were conducted for each sample.

3. RESULTS

3.1 Chemical composition

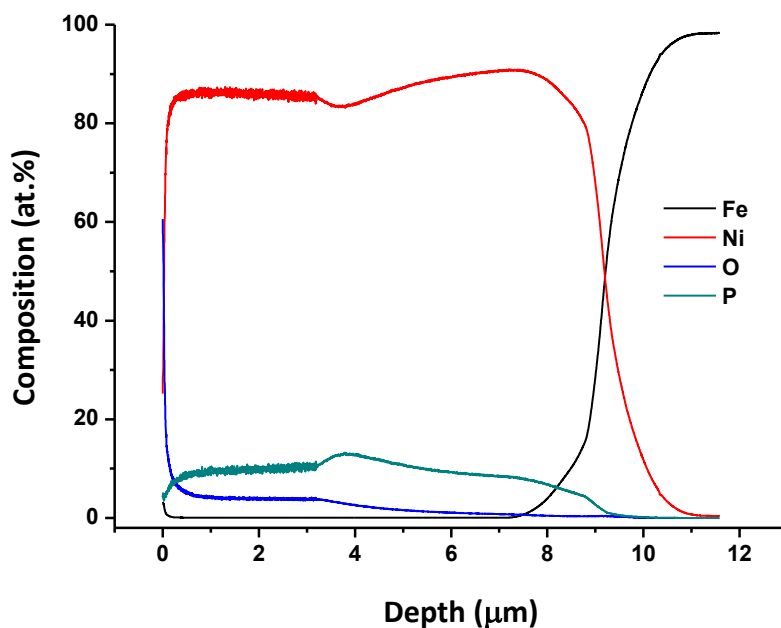


Figure 1. GDS elemental-distribution profiles of a Ni-P coating electrodeposited under galvanostatic conditions ($i = 30 \text{ mA}$, $t = 15 \text{ min}$) in solution S ($0.15 \text{ M H}_3\text{BO}_3$, 2 M NaCl , $0.65 \text{ M NiSO}_4 \cdot 6\text{H}_2\text{O}$, $0.75 \text{ M NiCl}_2 \cdot 6\text{H}_2\text{O}$, $0.10 \text{ M H}_3\text{PO}_3$, pH 1.5)

The electrodeposition of phosphorous (P) from an aqueous electrolyte on the cathode surface is possible only when the phosphorous is alloyed with another stable metal (i.e., Ni). The elemental composition profiles for the Ni-P coatings obtained under galvanostatic conditions ($i = 30 \text{ mA}$ and $t = 15 \text{ min}$) from solution S were determined with a GDS. Fig. 1 shows a typical elemental composition profile. The sample analysis was conducted at successive depths until the substrate (Fe) was reached. The thickness of the Ni-P deposit was approximately $10 \mu\text{m}$. A higher concentration of oxygen was present at the surface of the coating, presumably due to surface oxidation. After the oxide layer was removed from the surface, the relative concentrations of the elements Ni and P remained constant throughout the entire coating thickness: 87 at.% Ni and 10.6 at.% P, respectively. The presence of oxygen in the lower layers of the coating can be explained by the formation of nickel hydroxide in the interface metal/solution, as a result of the increased pH at the interface during the electrodeposition process [22].

3.2 Effect of the annealing temperature on thermal stability of the Ni-P (10.6 at.% P) coatings

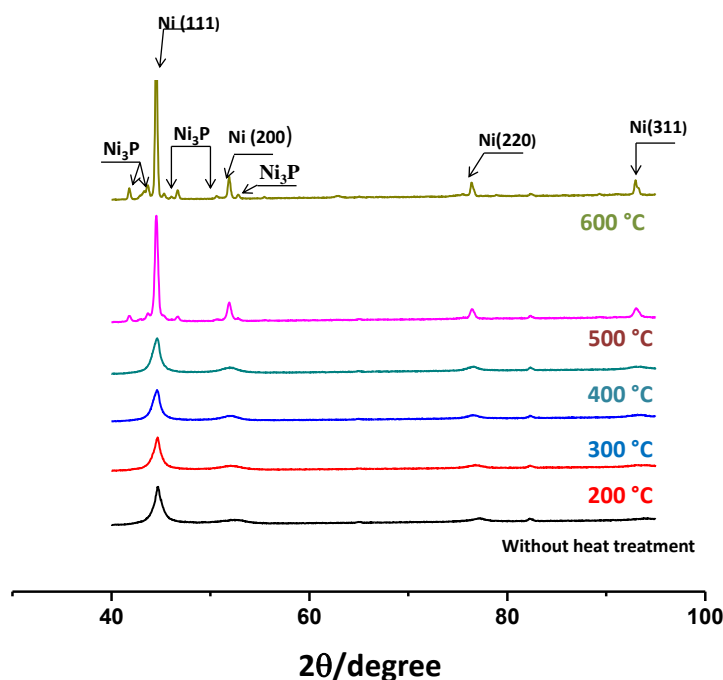
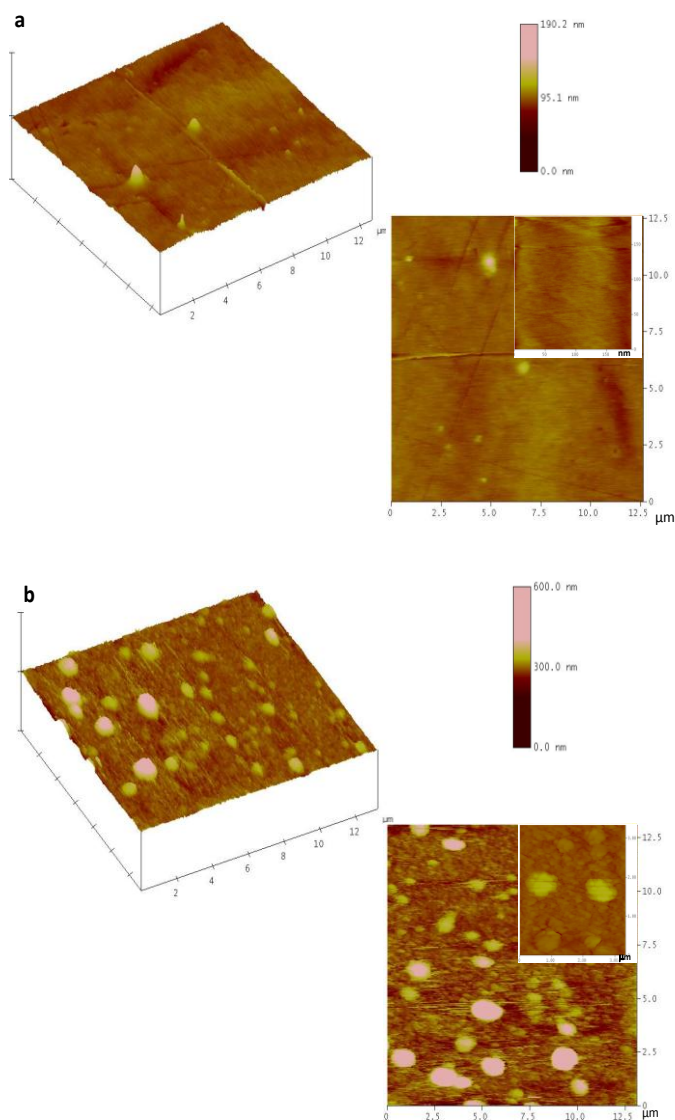


Figure 2. XRD patterns for Ni-P (10.6 at.% P) coatings electrodeposited onto AISI 1018 steel and heat treated at different temperatures. Ni (JCP2 04-0850) and Ni₃P (JCP2 89-2743).

Fig. 2 shows the XRD patterns for the Ni-P (10.6 at.% P) coatings both without and with heat treatment for 60 min at different temperatures. Only one broad peak could be distinguished in the X-ray diffraction patterns of the samples without heat treatment, indicating an amorphous structure [23]. There were no significant changes in the XRD patterns at annealing temperatures below $400 \text{ }^\circ\text{C}$, indicating that no phase transition occurred within this temperature range. When the heat treatment temperature was increased to $500 \text{ }^\circ\text{C}$, the structure became crystalline, and new peaks corresponding to

crystalline fcc Ni (JCP2 04-0850) and Ni₃P (JCP2 89-2743) appeared. This behavior can be attributed to the crystallization of pure nickel followed by the precipitation of nickel phosphide (Ni₃P) from the supersaturated nickel-phosphorous solid solution [6,24,25]. The onset of the allotropic transformation of the Ni-P alloy occurred between 400 and 500 °C. Studies of similar systems [26-28] have concluded that crystalline Ni-P alloys are denser than microcrystalline and amorphous alloys of the same chemical composition and that the transition from amorphous to crystalline structure is accompanied by a volume contraction [24].

Fig. 3 shows the AFM images obtained from Ni-P coatings thermally treated at three different temperatures: 400, 500, and 600 °C. When the coating was treated at 400 °C (Fig. 3a), an amorphous structure with a few crystals formed was observed; these crystals are associated with the initial formation of the Ni₃P species. At 500 °C (Fig. 3b), a larger quantity of crystals associated with the formation of the Ni₃P species was observed in addition to smaller crystals corresponding to fcc Ni. Finally, at 600 °C (Fig. 3c), the entire surface was covered with Ni₃P and Ni crystals. These results confirm the phase transition and formation of the Ni₃P and fcc Ni species observed by XRD.



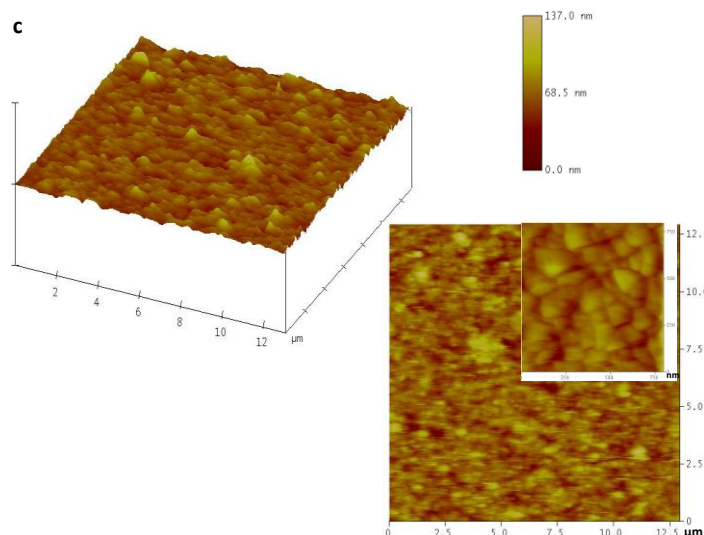


Figure 3. AFM images of Ni-P electrodeposited onto AISI 1018 steel under galvanostatic conditions ($i = 30 \text{ mA}$, $t = 15 \text{ min}$) in solution S and heat treated at different temperatures. (a) 400, (b) 500, and (c) 600 °C.

3.3 Microhardness of Ni-P (10.6 at.% P) electrodeposits

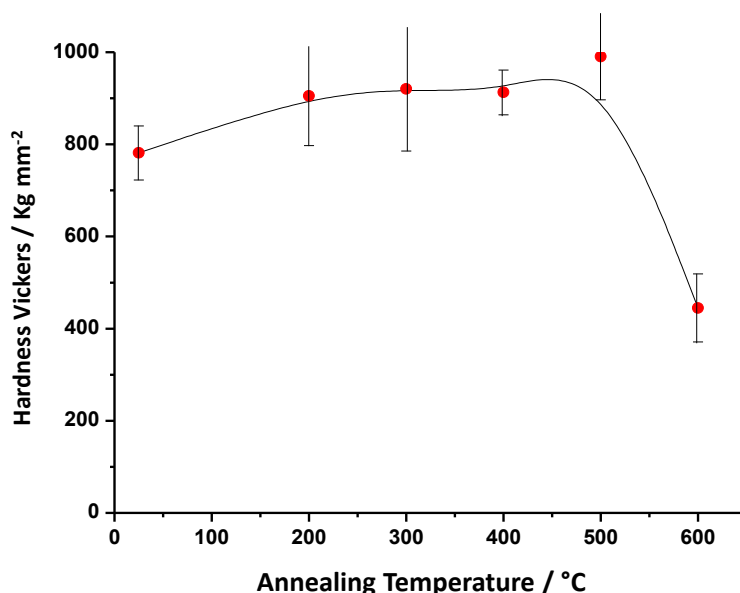


Figure 4. Hardness of the electrodeposited Ni-P (10.6 at.% P) coatings after a 60-min heat treatment.

The microhardness of the Ni-P coatings heat treated at various temperatures was measured. Fig. 4 illustrates the surface microhardness of the electrodeposited Ni-P coatings as a function of the annealing temperature. As observed from the curve, the hardness of the Ni-P coating depended on the annealing temperature in two ways. 1) When the annealing temperature was less than 500 °C, the hardness of the Ni-P alloy coatings increased slightly with increasing annealing temperature. A

significant increase in hardness from 908.2 HV to 998.8 HV was observed when the heat treatment was changed from 400 to 500 °C; this increase in hardness was associated with a structural change in the coating. Hard, intermetallic nickel phosphide (Ni_3P) particles begin to form within the amorphous nickel-phosphorus coating, hardening the precipitate. The hardness value of 990.0 Hv obtained at 500 °C is still slightly less than that of a hard chromium coating, which has a microhardness of 1020 HV [29]. 2) The hardness of the Ni-P alloy coating decreased drastically upon increasing the annealing temperature above 500 °C. At higher temperatures, the coating began to soften because the nickel phosphide particles conglomerate, reducing the number of hardening sites. This process also removes phosphorus from the alloy, producing a separate phase of soft nickel within the matrix and further reducing the bulk hardness.

3.4 Wear resistance

Fig. 5 shows the curves of the wear volume of the electrodeposited Ni-P coatings as a function of the annealing temperature. Once the coating began to harden at approximately 200 °C, the wear volume decreased drastically (i.e., the wear resistance increased drastically). The decrease in the wear volume at higher annealing temperatures was small. No significant changes were observed in the wear volume at temperatures above 500 °C. The coating that was heat treated at 600 °C contained cracks in its surface that could negatively influence its abrasion resistance.

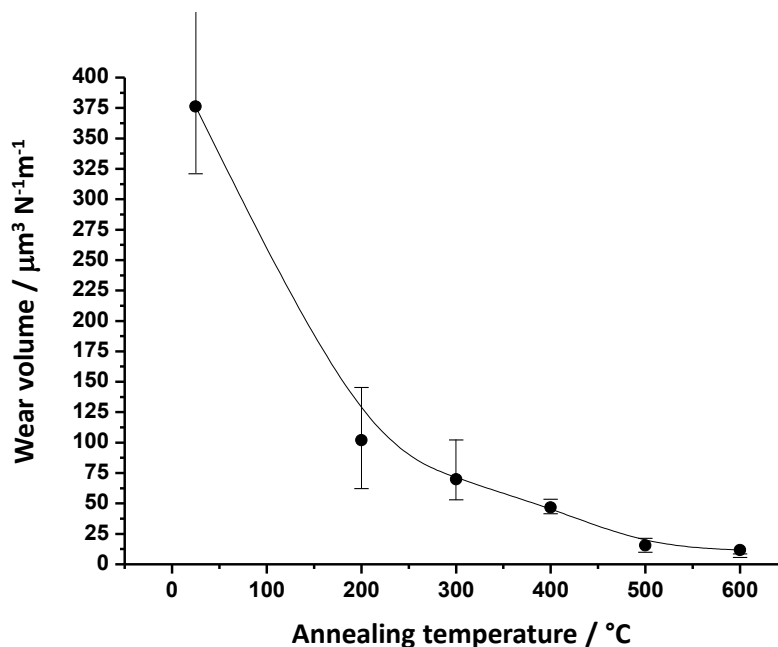


Figure 5. The wear volume of the Ni-P (10.6 at.% P) coatings after a 60-min heat treatment at different temperatures.

The relationship between the microhardness and wear volume of the Ni-P alloy electrodeposits was investigated before and after heat treatment at different temperatures. Fig. 6 shows that the wear

volume was inversely proportional to the microhardness of the deposits. In other words, a linear relationship exists between the hardness and wear resistance of the electrodeposited Ni-P coatings. Similarly, Jeong et al. [30] has proposed that the wear resistance of a material is proportional to its hardness under the same conditions.

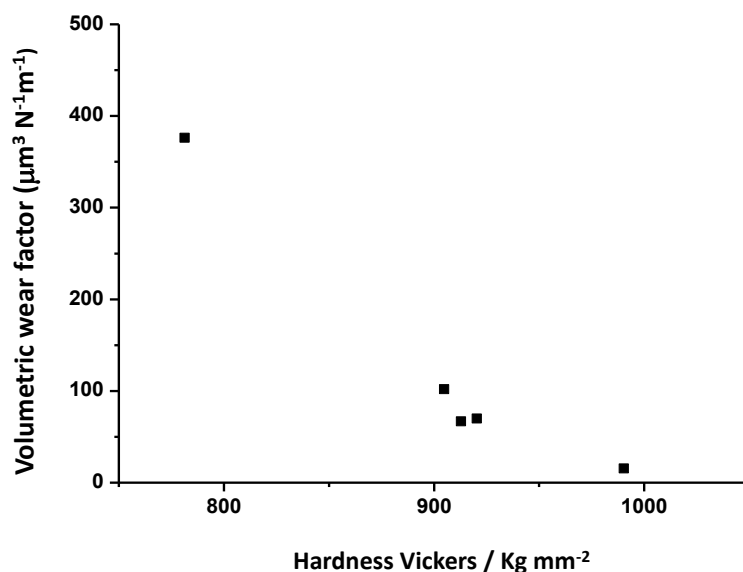


Figure 6. The relationship between the wear volume and the hardness of the Ni-P (10.6 at.% P) coatings after a 60-min heat treatment at different temperatures.

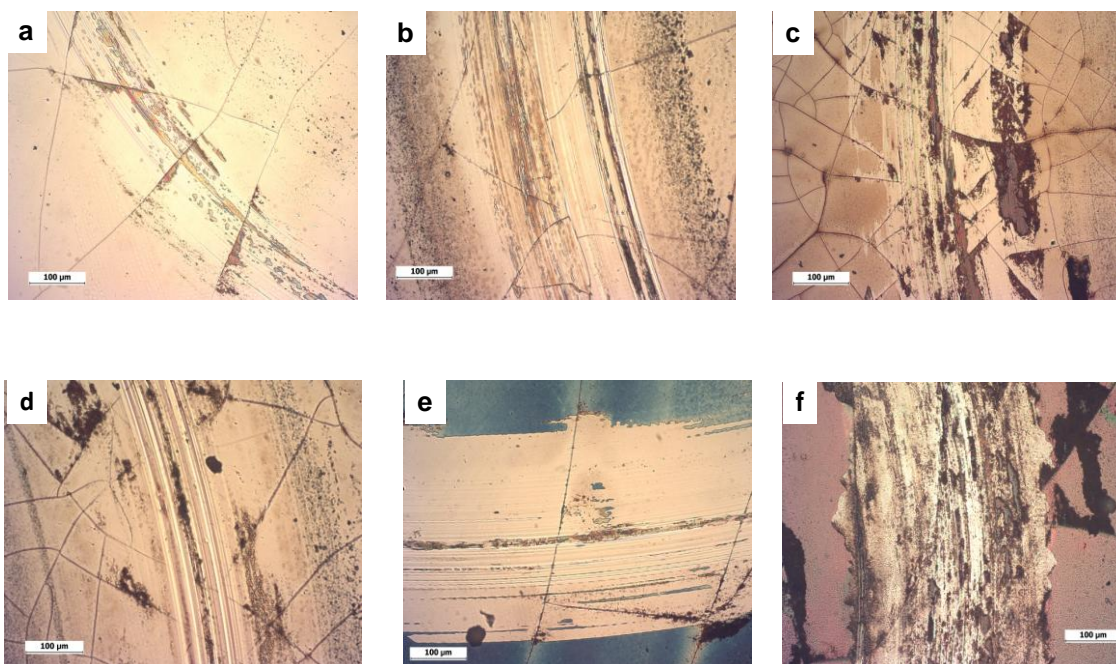


Figure 7. SEM images of wear track of Ni-P coatings, heat treated at different temperatures after sliding against AISI 8620 ball in air: a) without heat treatment, b) 200, c) 300, d) 400, e) 500, f) 600 °C

To understand the wear mechanism of the as-deposited Ni-P coatings treated at different temperatures, the wear track patterns were studied by SEM. As shown in Fig. 7, there were many adhesive tearing and plough lines in the sliding direction. Compared to the other Ni-P coatings, the coating treated at 500 °C exhibited the narrowest width and shallowest plough lines. These findings indicated that the coating treated at 500 °C had the best wear resistance.

3.5 Friction Coefficients

Fig. 8 shows the typical behavior for the friction coefficients of the Ni-P (10.6 at.% P) coatings both before and after heat treatment at different temperatures. The friction coefficients were obtained by sliding against an AISI 8620 ball at room temperature under non-lubricated conditions. Fig. 8 shows that when the Ni-P coatings (10.6 at.% P) were thermally treated at temperatures above 200 °C, the coefficient of friction rapidly reached equilibrium. After 1000 cycles, coatings treated at 500 °C had the lowest friction coefficient. In addition, the vibration amplitude of the friction coefficient was low for all of the coatings, indicating that the coatings exhibited relatively stable wear behavior.

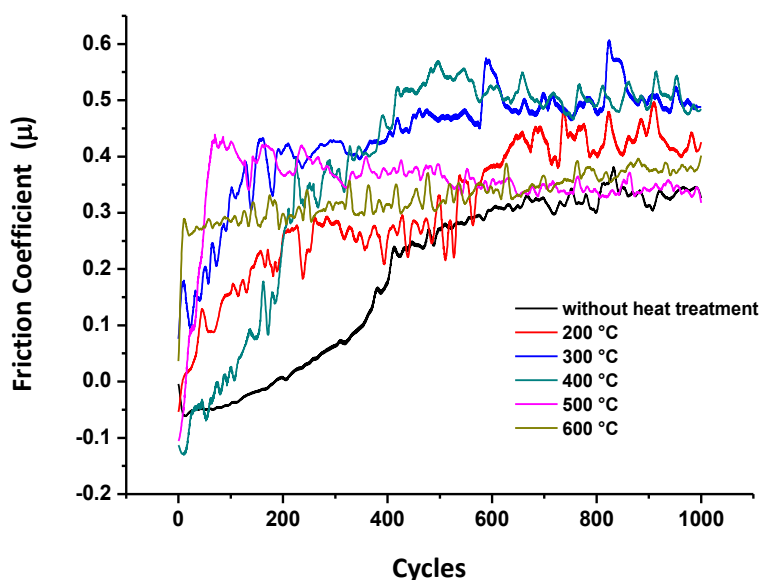


Figure 8. Frictional coefficient for the Ni-P (10.6 at.% P) coatings after a 60-min heat treatment at different temperatures.

3.6 Corrosion test

The Ni-P (10.6 at.% P) coatings were prepared on AISI 1018 steel electrodes with a geometric area of 1 cm² and then heat-treated at different temperatures, 400, 500 and 600 °C, for 1 h to evaluate their corrosion current density (j_{corr}). In all cases, the deposited thickness was approximately 10 μm, as measured by X-ray fluorescence.

The corrosion current density (j_{corr}) of each deposit was evaluated via the polarization curve technique using a 3 wt% NaCl solution (pH = 6.2); this solution is appropriate for studying corrosion because it contains corrosion activators (chloride ions). A potential scan ($v = 1.0 \text{ mV s}^{-1}$) was performed without stirring the solution by starting from a potential that was 300 mV more cathodic than the corrosion potential ($E_{initial} = E_{corr} - 300 \text{ mV}$) and scanning in the anodic direction. Prior to each experiment, the solution was saturated by bubbling with ultrapure nitrogen for 1 h. The resulting current was plotted against the potential on a logarithmic scale, and the corrosion current density (j_{corr}) was calculated according to the ASTM standards G 102 and G 59 [31,32].

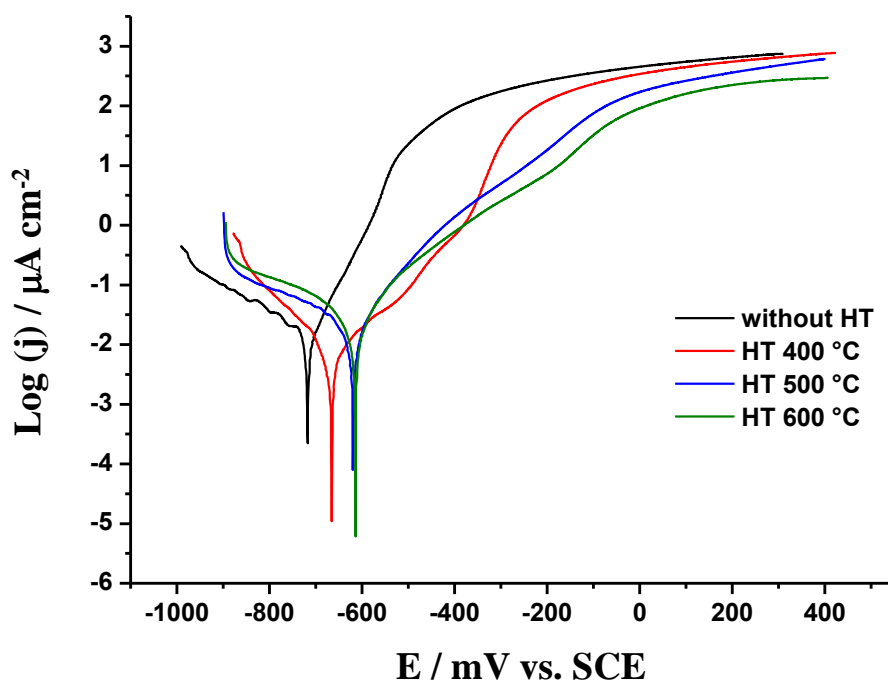


Figure 9. Polarization curves for the Ni-P coatings electrodeposited onto AISI 1018 steel in solution S and heat treated at different temperatures. $v = 0.166 \text{ mV s}^{-1}$.

Fig. 9 shows typical $\log(j)$ - E curves, measured in a 3 wt.% NaCl solution, for the deposited Ni-P (10.6 at.% P) both before and after the heat treatment in air. None of the curves in the anodic portion exhibit passive behavior, indicating that a passive film consisting primarily of nickel hydroxide is difficult to form in such media. The heat treatment positively affected the electrochemical behavior of the Ni-P (10.6 at.% P) coatings by deactivating the corrosion potential from -721.45 to -619.9 V vs. SCE after increasing the annealed temperature from 0 to 500 °C. When the heat treatment temperature was set to 600 °C, however, a less negative E_{corr} (-613.63 V vs. SCE) was obtained.

Table 1 summarizes the results obtained from the evaluation of the corrosion parameters of the coatings. The heat-treated Ni-P coatings possessed higher corrosion current density than the untreated coatings.

Table 1. Effects of heat treatment on the corrosion parameters of the Ni-P (10.6 at.% P) coatings.

Heat treatment temperature / °C	$E_{\text{corr.}}$ / mV vs. SCE	$j_{\text{corr.}}$ / $\mu\text{A cm}^{-2}$
Without heat treatment	-721.45	0.875
400	-664.12	0.838
500	-619.98	3.089
600	-613.67	4.685

The above results can be explained as follows: first, heat treatment favors the formation of Ni_3P , which is an intermetallic compound with high thermodynamic stability. Various studies [33,34] have shown that heat-treated Ni-P alloys produce a continuous Ni_3P layer with isolated areas containing nickel crystals, which make the alloy more resistant to corrosion. This resistance to localized corrosion is, however, limited in chloride media [5]. Second, heat treatment also favors the formation of Ni oxide on the surface of the deposit because the surface P is replaced by oxygen from the air after annealing [35]. In fact, the primary purpose of annealing in air is to form a uniform film of Ni-P and NiO on the deposit surface, which increases the anticorrosive capabilities of the Ni-P deposit, even though no passive response was detected for the annealed deposits. Third, the coatings that were treated with heat showed cracks in its surface, these cracks could influence on the values of its corrosion current density.

4. CONCLUSIONS

This work presents the results obtained from a study of the effects of thermal treatment on the tribological characteristics (hardness, wear resistance, and coefficient of friction) and corrosion resistance of electrodeposited Ni-P coatings (10.6 at.% P).

The XRD results indicated that the Ni-P alloy containing 10.6 at.% phosphorus was amorphous in nature. Thermal treatment between 400 and 500 °C changed the microstructure of the Ni-P matrix from amorphous to crystalline. Thermally treating the Ni-P coatings (10.6 at.% P) at temperatures ≥ 500 °C transformed the amorphous alloy into a continuous Ni_3P layer containing isolated nickel crystals.

An increased hardness and decreased wear coefficient were observed after heat treatment for 60 min at 500 °C due to the formation of a Ni_3P phase.

We also observed that the wear volume was inversely proportional to the microhardness of the deposits. In other words, a linear relationship existed between the hardness and wear resistance of the heat treated Ni-P alloy coatings. As a result, the Ni-P coatings (10.6% P) that were thermally treated at 500 °C possessed the greatest wear resistance.

The corrosion current density of the Ni-P coatings was increased by annealing in air. This behavior was associated with the formation of a cracked structure in the thermally treated coatings, which promotes localized corrosion.

References

1. R.L. Zeller, L. Salvati, *Corrosion* 50 (1994) 457.
2. M.C. Garcia-Alonso, M.L. Escudero, V. Lopez, A. Macias, *Corros. Sci.*, 38 (1996) 515.
3. Y.S. Huang, F.Z. Cui, *Surf. Coat. Tech.* 201 (2007) 5416.
4. S. Alirezaei, S.M. Monirvaghefi, M. Salehi, A. Saatchi, *Wear* 262 (2007) 978.
5. C.F. Malfatti, J. Zoppas Ferreira, C.B. Santos, B.V. Souza, E.P. Fallavena, S. Vaillant, J.P. Bonino, *Corrosion Sci.* 47 (2005) 567.
6. J.P. Bonino, S. Bruet-Hotellaz, C. Bories, P. Pouderoux, A. Rousset., *J. Appl. Electrochem.* 27 (1997) 1197.
7. D. Tachev, J. Georgieva, J. Armyanov, *Electrochim. Acta* 47 (2001) 359.
8. B. Bozzini, C. Martini, P.L. Cavallotti, E. Lanzoni, *Wear* 225-229 (1999) 806.
9. H. Kreye, R. Gutmann, *MetallOberfläche* 47 (1993) 387.
10. Chi-Chang Hu, A. Bai, *Materials Chemistry and Physics* 77 (2002) 215.
11. A. Bai, Chi-Chang Hu, *Materials Chemistry and Physics* 79 (2003) 49.
12. K.G. Keong, W. Sha, S. Malinov, *Surf. Coat. Tech.* 168 (2003) 263.
13. M. Crobu, A. Scorciapino, B. Elsener, A. Rossi, *Electrochim. Acta* 53 (2008) 3364.
14. J.L. He, M.H. Hon, *Surf. Coat. Technol.* 53 (1992) 93.
15. A. Sharma, A.K. Singh, *Cent. Eur. J. Eng.*, DOI 10.2478/s13531-011-0023-8
16. B. Bozzini, P.L. Cavallotti, G. Parisi, *British Corrosion Journal* 36 (2001) 49.
17. G. Lu, G. Zangari, *Electrochim. Acta* 47 (2002) 2969.
18. W. Sha, J. S. Pan, *J. Alloy Compd.*, 182 (1992) L1.
19. D.B. Lewis and G.W. Marshall, *Surf. Coat. Technol.* 78 (1996) 150.
20. A. Bai, P.Y. Chuang, Chi-Chang Hu, *Materials Chemistry and Physics* 82 (2003) 93.
21. L. Wang, Y. Gao, T. Xu, Q. Xue, *Appl. Surf. Sci.* 252 (2006) 7361.
22. K.H. Lee, D. Chang, S.C. Kwon, *Electrochim. Acta* 50 (2005) 4538.
23. D.B. Lewis, G.W. Marshall, *Surf. Coat. Technol.*, 78 (1996) 150.
24. C.F. Malfatti, J.Z. Ferreira, C.T. Oliveira, E.S. Rieder, J.P. Bonino, *Materials and Corrosion*, 63 (2012) 36.
25. T. Rabizadeh, S. Reza Allahkaram, A. Zarebidaki, *Materials and Design* 31 (2010) 3174.
26. K. Lu, M.L. Sui, R. Lück, *Nanostr. Mater.*, 4 (1994) 465
27. A. Serebryakov, V. Stelmukh, L. Voropaeva, N. Novokhatskaya, Yu. Levin, *Nanostr. Mater.*, 4 (1994) 645.
28. K. Lu, *Nanostr. Mater.*, 2 (1993) 643
29. S. Villant, L. Datas, J.P. Bonino, *Matér. Tech.* 89 (2001) 47.
30. D.H. Jeong, U. Erb, K.T. Aust, G. Palumbo, *Sct. Mater.*, 48 (2003) 1067.
31. 2004 Annual Book of ASTM Standards, Wear and Erosion; Metal Corrosion. P.C. Fazio et al. Editors, ASTM G102-89. Standard Practice for Calculation of Corrosion Rates and Related Information from Electrochemical Measurements, ASTM, Philadelphia, (2004)
32. 2003 Annual Book of ASTM Standards, Wear and Erosion; Metal Corrosion. P.C. Fazio et al. Editors, ASTM G59-97. Standard Test Method for Conducting Potentiodynamic Polarization Resistance Measurements, ASTM, Philadelphia, (2003)
33. H.G. Schenzel, H. Kreye, *Plat. Surf. Finish.*, 77 (1990) 50
34. B. Gillot, K. El Amri, P. Pouderoux, J.P. Bonino, A. Rousset, *J. Alloys Comp.* 189 (1992) 151
35. R.N. Duncan, *Metal Finish.*, 88 (3) (1990) 11